Inorg. Chem. **2004**, *43*, 8637–8648

Tetra-2,3-pyrazinoporphyrazines with Externally Appended Pyridine Rings. 2. Metal Complexes of Tetrakis-2,3-[5,6-di(2-pyridyl)pyrazino]porphyrazine: Linear and Nonlinear Optical Properties and Electrochemical Behavior

Maria Pia Donzello,[†] Zoungping Ou,[‡] Danilo Dini,[§] Moreno Meneghetti,[||] Claudio Ercolani,*[,†] and Karl M. Kadish*[,‡]

Dipartimento di Chimica, Università degli Studi di Roma "La Sapienza", P.le A. Moro 5, I-00185 Roma, Italy, Department of Chemistry, University of Houston, Houston, Texas 77204-5003, Institute of Organic Chemistry, University of Tübingen, Auf der Morgenstelle 18, D-72076 Tübingen, Germany, and Dipartimento di Chimica Fisica, Università di Padova, Via Loredan 2, I-35131 Padova, Italy

Received August 9, 2004

A series of metal complexes of tetrakis-2,3-[5,6-di(2-pyridyl)pyrazino]porphyrazine, [$Py_8TPyzPzH_2$], having the general formula [$Py_8TPyzPzM$]·xH_2O (M = $Mg^{II}(H_2O)$, Mn^{II}, Co^{II}, Cu^{II}, Zn^{II}; x = 3–8) were synthesized by reaction of the free-base macrocycle with the appropriate metal acetate in pyridine or dimethyl sulfoxide under mild conditions. Clathrated water and retained pyridine molecules for the Mn^{II} and Co^{II} species are easily eliminated by heating under vacuum, the water molecules being recovered by exposure of the unsolvated macrocycles to air. Magnetic susceptibility measurements and EPR spectra of the materials in the solid state provide basic information on the spin state of the Cu^{II}, Co^{II}, and Mn^{II} species. Colloidal solutions caused by molecular aggregation are formed in nondonor solvents (CH_2Cl_2, $CHCl_3$), a moderately basic solvent (pyridine), and an acidic solvent (CH_3COOH), with the extent of aggregation depending on the specific solvent and the central metal ion. UV–vis spectral monitoring of the solutions after preparation indicates that disaggregation systematically occurs as a function of time leading ultimately to the formation of clear solutions containing the monomeric form of the porphyrazine. Cyclic voltammetry and thin-layer spectroelectrochemistry show that each compound with an electroinactive metal ion undergoes four reversible one-electron reductions, leading to formation of the negatively charged species [$Py_8TPyzPzM$]$^{n-}$ (n = 1 − 4). The stepwise uptake of four electrons is consistent with a ring-centered reduction, but in the case of the cobalt complex a metal-centered ($Co^{II} \rightarrow Co^{I}$) reduction occurs in the first process and only three additional reductions are observed. No oxidations are observed in pyridine or CH_2Cl_2 containing 0.1 M tetrabuthylammonium perchlorate (TBAP). The nonlinear optical properties (NLO) of the species [$Py_8TPyzPzM$] (M = $2H^{I}$, Cu^{II}, Zn^{II}, $Mg^{II}(H_2O)$) have also been examined with nanosecond pulses at 532 nm in dimethyl sulfoxide solution. Reverse saturable absorption is shown by all of the [$Py_8TPyzPzM$] species, which exhibit distinct behavior depending on the nature of M and extent of aggregation.

Introduction

The previous paper in this series[1] reports the synthesis and characterization of tetrakis-2,3-[5,6-di(2-pyridyl)pyrazino]-porphyrazine, [$Py_8TPyzPzH_2$]. The four external dipyridinopyrazine fragments significantly enhance the overall electron-deficiency properties of the entire macrocycle through σ and π bond mechanisms of charge transmission, with relevant effects on the acidity strength of the neutral macrocycle [$Py_8TPyzPzH_2$], leading to facile multistep one-electron reductions for both [$Py_8TPyzPzH_2$] and its corresponding dianion [$Py_8TPyzPz$]$^{2-}$.[1]

* To whom correspondence should be addressed. E-mail: claudio.ercolani@uniromal.it (C.E.); kkadish@uh.edu (K.M.K.).
[†] Università degli Studi di Roma "La Sapienza".
[‡] University of Houston.
[§] University of Tübingen.
[||] Università di Padova.

(1) Part 1: Donzello, M. P.; Ou, Z.; Monacelli, F.; Ricciardi, G.; Rizzoli, C.; Ercolani, C.; Kadish, K. M. *Inorg. Chem.* **2004**, *43*, 8626−8636.

10.1021/ic0489084 CCC: $27.50
Published on Web 12/03/2004

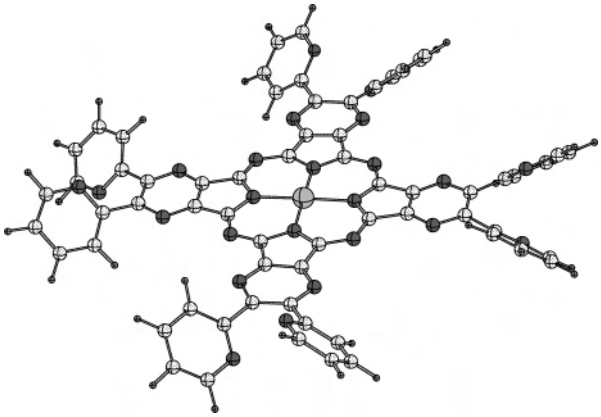

Figure 1. Schematic arbitrary representation of the macrocycle [$Py_8TPyzPzM$].

This paper extends our studies to include metal complexes with the same easily reduced macrocycle. The investigated compounds have the general formula [$Py_8TPyzPzM$]·xH_2O ($x = 3-8$), M being a bivalent nontransition metal (Mg^{II}) or a first-row transition metal ion (Mn^{II}, Co^{II}, Cu^{II}, Zn^{II}) (Figure 1). Information on the stability, general physicochemical properties, and redox behavior of the compounds was obtained on these species by IR, UV−vis and EPR spectra, magnetic susceptibility, and electrochemical and spectroelectrochemical measurements.

Owing to our growing interest in the examination of the nonlinear optical (NLO) behavior of related novel classes of porphyrazines,[2] nonlinear transmission measurements on the nanosecond time scale were also carried out in DMSO for some of the [$Py_8TPyzPzM$]·xH_2O complexes. The macrocycles show multiphoton absorption, which implies a reverse saturable absorption mechanism. The data are presented and discussed in the framework of this mechanism.

Experimental Section

Solvents and chemicals were reagent grade and were used as received, with a few exceptions. Pyridine was normally freshly distilled over barium oxide before use. DMSO was predistilled over calcium hydride. The precursor 2,3-dicyano-5,6-di(2-pyridyl)-1,4-pyrazine, [$(CN)_2Py_2Pyz$], and the free-base macrocycle [$Py_8TPyzPzH_2$]·$2H_2O$ were prepared as reported in part 1.[1]

Synthesis. Similar procedures were used for synthesis of [$Py_8TPyzPzM$]·xH_2O. A detailed description is given below for M = $Mg^{II}(H_2O)$ and this is followed by more concise presentations for the complexes where M = Mn^{II}, Co^{II}, Cu^{II}, and Zn^{II}.

Hydrated Tetrakis-2,3-[5,6-di(2-pyridyl)pyrazino]porphyrazinato(monoaquo)magnesium(II), [$Py_8TPyzPzMg(H_2O)$]·xH_2O ($x = 4-6$). A mixture of [$Py_8TPyzPzH_2$]·$2H_2O$ (303 mg, 0.26 mmol) and $Mg(OCOCH_3)_2$·$4H_2O$ (280 mg, 1.30 mmol) in pyridine (6 mL) was kept refluxing for 4 h. After cooling, the brilliant green solid formed was separated by centrifugation, washed repeatedly with water to remove the unreacted Mg^{II} acetate, and then with acetone, and brought to constant weight under vacuum (10^{-2} mmHg) (183 mg, yield 55%). Calcd for [$Py_8TPyzPzMg(H_2O)$]·$4H_2O$, $C_{64}H_{42}MgN_{24}O_5$: C, 61.42; H, 3.38; N, 26.86. Found: C, 61.68; H, 3.28; N, 26.84%. MS (FAB), *m*/*z* (%): 1161 (100) $[Py_8TPyzPzMg]^+$. IR (cm^{-1}): 3055 w, 3003 vw, 1637 m, 1586 s, 1568 s, 1548 m, 1473 s, 1434 m, 1412 sh, 1385 vw, 1360 vs, 1292 w, 1246 vs, 1193 s, 1152 w, 1113 s, 1080 m, 1048 w, 994 s, 956 vs, 897 vw, 865 w, 830 m, 789 s, 749 s, 714 vs, 679 vw, 662 m, 630 w, 619 sh, 605 vw, 584 vw, 557 m, 507 vw, 469 sh, 439 m, 405 w. TGA shows a weight loss of 5.25% in the range 25−100 °C (calcd for four molecules of water: 5.76%). Similarly, the Mg^{II} complex was also obtained in DMSO (2 mL) from [$Py_8TPyzPzH_2$]·$2H_2O$ (50 mg, 0.042 mmol) and $Mg(OCOCH_3)_2$·$(H_2O)_4$ (52 mg, 0.24 mmol); $T = 120$ °C, $t = 4$ h (29 mg, yield 53%).

The Mg^{II} complex could be also prepared by template cyclotetramerization of [$(CN)_2Py_2Pyz$] in the presence of magnesium amylate: magnesium metal (150.9 mg, 6.21 mmol) was suspended, with stirring, in amyl alcohol (20 mL) in the presence of a small amount of I_2, and the mixture was refluxed for 16 h to complete the conversion of Mg into its corresponding amylate. The precursor [$(CN)_2Py_2Pyz$] (399.6 mg, 1.41 mmol) was then added and the mixture kept refluxing for another 10 h. During the reaction, the gray mixture changed to dark green, and then to dark blue. At the end of the reaction, amyl alcohol was evaporated under reduced pressure, and the solid material was washed with acetone to remove the unreacted monomer. The ground solid was suspended in 50% aqueous acetic acid and stirred for 30 min at room temperature to dissolve the residual unchanged magnesium amylate. This last step of the procedure does not result in a demetalation of the complex. The dark blue solid, separated by centrifugation, was washed with water to neutrality and dried under vacuum (10^{-2} mmHg) (153 mg, yield 30%). Calcd for [$Py_8TPyzPzMg(H_2O)$]·$6H_2O$, $C_{64}H_{46}MgN_{24}O_7$: C, 59.70; H, 3.60; N, 26.11. Found: C, 59.52; H, 2.96; N, 25.44%.

Hydrated Tetrakis-2,3-[5,6-di(2-pyridyl)pyrazino]porphyrazinato-manganese(II), [$Py_8TPyzPzMn$]·xH_2O ($x = 3-5$). A mixture of [$Py_8TPyzPzH_2$]·$2H_2O$ (298 mg, 0.25 mmol) and $Mn(OCOCH_3)_2$·$4H_2O$ (310 mg, 1.26 mmol) was heated in pyridine (6 mL; reflux, $t = 2$ h, under N_2). The solid obtained was separated, washed with water and acetone, and brought to constant weight under vacuum (10^{-2} mmHg) (220 mg, yield 71%). This material was shown to contain pyridine, which was eliminated by heating at 150 °C for 2 h under vacuum (10^{-2} mmHg). The sample was then stabilized in air. Calcd for [$Py_8TPyzPzMn$]·$3H_2O$, $C_{64}H_{38}MnN_{24}O_3$: C, 61.69; H, 3.01; N, 26.98. Found: C, 61.19; H, 2.96; N, 26.50%. MS (FAB), *m*/*z* (%): 1192 (100) $[Py_8TPyzPzMn]^+$. IR (cm^{-1}): 3040 vw, 1679 w, 1628 w, 1585 m, 1566 w, 1544 w, 1505 vw, 1470 m, 1434 w, 1418 sh, 1383 vw, 1356 vs, 1317 m, 1297 sh, 1239 vs, 1183 w, 1138 m, 1122 sh, 1092 w, 1046 w, 993 s, 965 s, 904 vw, 875 vw, 826 m, 785 vs, 747 s, 714 vs, 662 w, 631 w, 599 vw, 577 vw, 554 m, 529 vw, 518 vw, 508 vw, 482 sh, 460 vw, 443 vw, 435 w, 426 vw, 417 w, 412 sh, 403 m. TGA shows a loss of three water molecules in the range 25−100 °C (found 3.79%, calcd 4.34%). The reaction could also be conducted at room temperature with stirring for 24 h.

The Mn^{II} complex could also be prepared in DMSO (2 mL) from [$Py_8TPyzPzH_2$]·$2H_2O$ (58.5 mg, 0.050 mmol) and $Mn(OCOCH_3)_2$·$4H_2O$ (89.3 mg, 0.36 mmol); $T = 120$ °C, $t = 3$ h, under N_2 (25.6 mg, yield 40%).

Hydrated Tetrakis-2,3-[5,6-di(2-pyridyl)pyrazino]porphyrazinato-cobalt(II), [$Py_8TPyzPzCo$]·xH_2O ($x = 3-8$). The complex was prepared by refluxing in pyridine (8 mL) a mixture of [$Py_8TPyzPzH_2$]·$2H_2O$ (250 mg, 0.21 mmol) and $Co(OCOCH_3)_2$·$4H_2O$ (250 mg, 1.00 mmol) for 3 h. The solid obtained was separated, washed (water, acetone), and dried (178 mg, yield 68%).

(2) (a) Donzello, M. P.;Dini, D.; D'Arcangelo, G.; Ercolani, C.; Zhan, R.; Ou, Z.; Stuzhin, P. A.; Kadish, K. M. *J. Am. Chem. Soc.* **2003**, *125*, 14190. (b) Donzello, M. P.; Ercolani, C.; Gaberkorn, A. A.; Kudrik, E. V.; Meneghetti, M.; Marcolongo, G.; Rizzoli, C.; Stuzhin, P. A. *Chem. Eur. J.* **2003**, *9*, 4009.

The complex was shown to contain pyridine, which was eliminated by heating at 150 °C for 2 h under vacuum (10^{-2} mmHg). The sample was then re-exposed to air. Calcd for $[Py_8TPyzPzCo]\cdot 3H_2O$, $C_{64}H_{38}CoN_{24}O_3$: C, 61.49; H, 3.06; N, 26.89. Found: C, 60.96; H, 2.86; N, 26.77%. MS (FAB), *m*/*z* (%): 1196 (100) $[Py_8TPyzPzCo]^+$. IR (cm^{-1}): 3049 vw, 1632 w, 1585 m, 1560 s, 1526 m, 1470 m, 1436 w, 1416 vw, 1385 vw, 1358 s, 1343 s, 1294 vw, 1246 vs, 1193 m, 1131 vs, 1107 w, 1097 m, 1046 vw, 1016 vw, 994 s, 971 s, 955 sh, 900 vw, 880 vw, 829 m, 790 s, 755 s, 748 sh. 723 w, 714 vs, 690 sh, 663 w, 651 sh, 630 w, 604 vw, 586 vw, 556 m, 535 vw, 526 vw, 503 w, 488 vw, 440 w, 426 vw, 417 vw. TGA shows a loss of three molecules of water in the range 25−100 °C (found 3.74%, calcd 4.32%). The same complex can be obtained at room temperature with stirring for 24 h.

Alternatively, the Co^{II} complex could be prepared in DMSO (5 mL) by heating a mixture of $[Py_8TPyzPzH_2]\cdot 2H_2O$ (250 mg, 0.21 mmol) and $Co(OCOCH_3)_2\cdot 4H_2O$ (250 mg, 1.00 mmol) at 100 °C for 2 h (170 mg, yield 63%).

Hydrated Tetrakis-2,3-[5,6-di(2-pyridyl)pyrazino]porphyrazinato-copper(II), $[Py_8TPyzPzCu]\cdot xH_2O$ ($x = 3-7$). A mixture of $[Py_8TPyzPzH_2]\cdot 2H_2O$ (299 mg, 0.25 mmol) and $Cu(OCOCH_3)_2\cdot H_2O$ (273 mg, 1.50 mmol) in pyridine (6 mL) was kept refluxing for 4 h. The amount of complex obtained after separation, repeated washing, and drying was 179 mg (yield 56%). Calcd for $[Py_8TPyzPzCu]\cdot 4H_2O$, $C_{64}H_{40}CuN_{24}O_4$: C, 60.40; H, 3.17; N, 26.41. Found: C, 60.35; H, 2.71; N, 25.86%. MS (FAB), *m*/*z* (%): 1200 (100) $[Py_8TPyzPzCu]^+$. IR (cm^{-1}): 3056 vw, 1632 w, 1586 m, 1566 w, 1555 m, 1508 m, 1467 m, 1463 m, 1432 w, 1385 vw, 1360 s, 1293 w, 1246 s, 1198 m, 1149 w, 1122 s, 1092 m, 1046 w, 994 s, 964 vs, 898 vw, 865 w, 830 m, 787 vs, 750 vs, 712 vs, 661 s, 630 w, 619 sh, 604 vw, 555 s, 535 vw, 512 vw, 498 w, 481 vw, 470 sh, 438 s, 406 w. TGA shows a weight loss of 5.55% in the range 25−100 °C (calcd for four molecules of water 5.66%). The same product could also be obtained by stirring the reaction mixture at room temperature for 24 h.

The synthesis of the complex was also conducted in DMSO by reaction of $[Py_8TPyzPzH_2]\cdot 2H_2O$ (53 mg, 0.045 mmol) and $Cu(OCOCH_3)_2\cdot H_2O$ (51 mg, 0.28 mmol) (RT, 24−48 h; 18 mg, yield 33%).

The Cu^{II} complex could also be prepared by heating the precursor $[(CN)_2Py_2Pyz]$ in the presence of metallic copper as follows: A thick test tube containing powdered Cu (500 mg, 7.87 mmol) was immersed in an oil bath at 180 °C. $[(CN)_2Py_2Pyz]$ (385 g, 1.35 mmol) was added, and the mixture was manually stirred until it almost completely solidified (1 h). After cooling, the solid material was finely ground and purified by extraction in a Soxhlet with CH_3OH and then with pyridine. The pyridine solution was brought to dryness and the green solid residue brought to a constant weight under vacuum (10^{-2} mmHg) (320 mg). The product was further purified by suspension in pyridine (2 mL) and refluxing for 3 h. After cooling, the brilliant green solid was separated by centrifugation and brought to constant weight under vacuum (90 mg, yield 20%). Calcd for $[Py_8TPyzPzCu]\cdot 7H_2O$, $C_{64}H_{46}CuN_{24}O_7$: C, 57.94; H, 3.49; N, 25.34. Found: C, 58.10; H, 3.33; N, 25.04%.

Hydrated Tetrakis-2,3-[5,6-di(2-pyridyl)pyrazino]porphyrazinato-zinc(II), $[Py_8TPyzPzZn]\cdot xH_2O$ ($x = 5-7$). A mixture of $[Py_8TPyzPzH_2]\cdot 2H_2O$ (302 mg, 0.26 mmol) and $Zn(OCOCH_3)_2\cdot 2H_2O$ (302 mg, 1.37 mmol) in pyridine (6 mL) was kept refluxing for 4 h. The amount of complex obtained as a pure solid was 211 mg (yield 65%). Calcd for $[Py_8TPyzPzZn]\cdot 5H_2O$, $C_{64}H_{42}N_{24}O_5Zn$: C, 59.47; H, 3.28; N, 26.01. Found: C, 59.31; H, 3.06; N, 25.22%. MS (FAB), *m*/*z* (%): 1203 (100) $[Py_8TPyzPzZn]^+$. IR (cm^{-1}): 3045 vw, 3010 vw, 2923 w, 2854 w, 1773 vw, 1749 vw, 1733 vw, 1719 vw, 1699 vw, 1654 m, 1622 m, 1579 m, 1557 vw, 1542 w, 1515 w, 1509 w, 1490 w, 1473 vw, 1457 w, 1434 w, 1407 vw, 1386 w, 1357 s, 1320 sh, 1280 w, 1243 vs, 1189 m, 1146 w, 1109 s, 1090 m, 1045 sh, 1021 sh, 994 m, 954 s, 904 sh, 853 w, 827 w, 788 sh, 777 m, 744 s, 700 vs, 655 s, 625 w, 602 vw, 568 w, 553 w, 506 w, 473 vw, 436 m. TGA shows a loss of five molecules of water in the range 25−100 °C (found ca. 6.30%, calcd 6.97%). The same product could also be obtained by stirring the reaction mixture at room temperature for 30 h.

The Zn^{II} complex was also prepared in DMSO (4 mL) by heating a mixture of $[Py_8TPyzPzH_2]\cdot 2H_2O$ (250 mg, 0.21 mmol) and $Zn(OCOCH_3)_2\cdot 2H_2O$ (300 mg, 1.37 mmol) at 100 °C for 6 h (172 mg, yield 65%). At room temperature the same reaction arrives to completion in 24−48 h.

The zinc complex could also be prepared by reaction of the precursor $[(CN)_2Py_2Pyz]$ with the metal acetate, with a procedure similar to that reported above for the Cu^{II} complex (yield 16%). Calcd for $[Py_8TPyzPzZn]\cdot 7H_2O$, $C_{64}H_{46}N_{24}O_7Zn$ (MW = 1328.61): C, 57.86; H, 3.49; N, 25.30. Found: C, 57.95; H, 3.36; N, 24.77%. TGA shows a weight loss of 9.40% in the range 25−100 °C (calcd for 7 molecules of water 9.49%).

Electrochemical and Spectroelectrochemical Measurements. Cyclic voltammetric (CV) measurements were performed at 298 K on an EG&G model 173 potentiostat coupled with an EG&E model 175 universal programmer in CH_2Cl_2 (Fluka) or pyridine (Aldrich, anhydrous, 99.8%) solution containing 0.1 M tetrabutylammonium perchlorate (TBAP) as supporting electrolyte. High purity N_2 from Trigas was used to deoxygenate the solution before each electrochemical experiment. TBAP was purchased from Sigma Chemical or Fluka Chemika Co., recrystallized from ethyl alcohol, and dried under vacuum at 40 °C for at least one week prior to use. A three electrode system was used and consisted of a glassy carbon working electrode, a platinum wire counter electrode, and a saturated calomel reference electrode (SCE). The reference electrode was separated from the bulk solution by a fritted-glass bridge filled with the solvent, supporting electrolyte mixture. Thin-layer spectroelectrochemistry measurements were carried out at an optically transparent platinum thin-layer working electrode using a Hewlett-Packard model 8453 diode array spectrophotometer coupled with an EG&G model 173 universal programmer. These measurements were carried out in solutions containing 0.2 M TBAP as supporting electrolyte. Parallel EPR spectra were obtained with an IBM model ESP 300 apparatus.

Nonlinear Optical Measurements. Nonlinear transmission measurements were obtained with 10 ns pulses of a Nd:YAG laser (Quantel YG980E) at its duplicated frequency (532 nm). Fluence (F) was varied in the range $10 \leq F \leq 1300$ mJ cm^{-2}. Measurements of the incident and transmitted energies were carried out pulse by pulse with a pyroelectric detector (Scientech SPHD25) and a calibrated photodiode. A half-wave plate and a cube polarizer were used for controlling the pulse energies. Glass cuvettes with 2 mm optical path length were used for the 0.1 mM solutions in DMSO. The laser beam diameter on the sample was of the order of 2.5 mm. Associated linear optical spectra were recorded with a UV−vis−NIR spectrometer (Varian Cary 5) before and after the nonlinear trasmission measurements.

Other Physical Measurements. IR spectra were taken with a Perkin-Elmer 1760 X spectrophotometer in the range 4000−400 cm^{-1} by using KBr pellets. UV−vis solution spectra other than those for spectroelectrochemistry (see above) were recorded with a Varian Cary 5E spectrometer. Thermogravimetric analyses (TGA) were performed on a Stanton Redcroft model STA-781 analyzer

Scheme 1

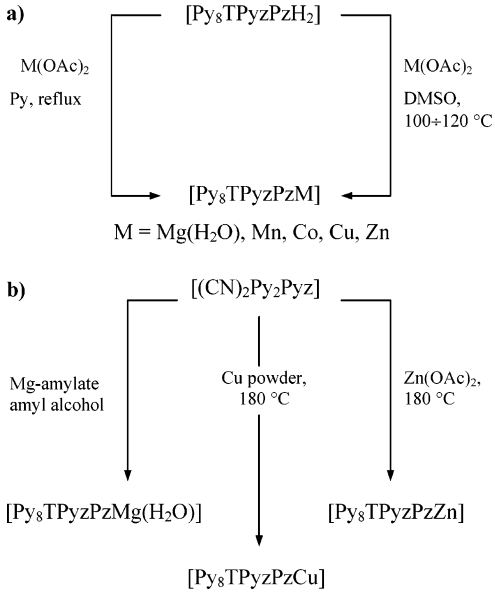

under a N_2 atmosphere (0.5 L/min). FAB experiments were carried out on a multiple quadrupole instrument (VG quattro). Elemental analyses for C, H, and N were provided by the "Servizio di Microanalisi" at the Dipartimento di Chimica, Università "La Sapienza" (Rome), on an EA 1110 CHNS-O instrument. X-ray powder diffraction patterns were obtained on a Philips PW 1710 diffractometer by using Cu Kα (Ni-filtered) radiation. Room temperature magnetic susceptibility measurements were carried out by the Gouy method using a $NiCl_2$ solution as calibrant. The low temperature (80 K) EPR spectra were recorded on a Varian V 4502-4 spectrometer, at the Dipartimento di Chimica, Università "La Sapienza" (Rome).

Results and Discussion

Preparative Aspects. On the basis of our results, it was established that metal complexes having the formula $[Py_8TPyzPzM]\cdot xH_2O$ ($M = Mg^{II}(H_2O)$, Mn^{II}, Co^{II}, Cu^{II}, Zn^{II}; $x = 3-8$) can be prepared, generally in fairly good yield, all by the following procedures (Scheme 1): (a) reaction of the hydrated free-base macrocycle $[Py_8TPyzPzH_2]\cdot 2H_2O$ with M^{II}−acetate in py or DMSO; (b) cyclotetramerization of the precursor $[(CN)_2Py_2Pyz]$ in the presence of the metal acetate (Zn) or amylate (Mg), or by reaction with metallic powder (for Cu, more laborious purification required).

The observed systematic presence of clathrated water molecules (hereafter neglected in the formulas given, unless specifically required) parallels what is observed for the corresponding free-base macrocycle,[1] closely related aza analogues,[2,3] and porphyrazines in general.[4] Although the presence of water is given as a specific number for each complex in the Experimental Section, it was verified that the water content can vary significantly for different batches of each metal complex. The Mg^{II} complex is formulated with one water molecule directly ligated to the metal, i.e., $[Py_8TPyzPzMg(H_2O)]$. This is an assumption made also for the previously reported Mg^{II} complexes of tetrakis(thia/selenodiazole)porphyrazine[3a,c] and tetrakis-2,3-(5,7-diphenyl-6*H*-diazepino)porphyrazine,[3e,2a] given some support by experimental data and also strongly suggested by the structures of the tetrapyrrolic macrocycles $[PcMg(H_2O)]\cdot 2py$[5] and (aquo)(octakis(methylthio)porphyrazinato)magnesium(II) $[(omtp)Mg(H_2O)]$;[6] interestingly, even a bis-hydrate of PcMg has been reported,[7] and a dimerized monohydrate of a low-symmetry porphyrazine macrocycle has been structurally elucidated.[8]

The Mn^{II} and Co^{II} complexes normally retain some pyridine if prepared from this solvent. In our experience, however, the observed presence of pyridine molecules in the complex was found to vary from sample to sample in the range 0.5−2 mol per mol of complex. Thus, no fixed stoichiometry could be definitely established. Evidently, the pyridine molecules do not bind strongly to the metal center of the Mn^{II} and Co^{II} complexes, and drying of the solid under vacuum leads to some releasing of the N-base. A mere dispersion of pyridine in the solid is believed to be improbable. Thermogravimetric analyses show that all the metal complexes, once desolvated (loss of pyridine in the range 100−200 °C), are stable in an inert atmosphere up to ca. 300 °C or slightly above. Exposure of the heated samples to air leads to rehydration of the materials.

Solid State Properties. Magnetic Susceptibility and EPR Data. Basic information on the electronic spin state of the Cu^{II}, Co^{II}, and Mn^{II} complexes was obtained by magnetic susceptibility and EPR measurements. These data are shown in Table 1 together with data for some of the previously reported porphyrazine analogues.[3b,d,2a]

The magnetic data for the complexes $[Py_8TPyzPzM]$ highly depend on the accuracy of the measured diamagnetic contribution of the entire macrocycle owing to its high molecular weight. The molar susceptibility directly measured for the diamagnetic bis-hydrated Zn^{II} complex, $[Py_8TPyzPzZn]\cdot 2H_2O$, is -650×10^{-6} cgsu, in excellent agreement with the value measured for the hydrated free-base ligand, $[Py_8TPyzPzH_2]\cdot 2H_2O$, i.e. -629×10^{-6} cgsu.[1] Thus, the value for the Zn^{II} complex was used for estimating the diamagnetic contribution present in the other metal complexes ($M = Mn^{II}$, Co^{II}, Cu^{II}) after making appropriate corrections, with Pascal's constants,[9] for the different metal centers and number of water molecules in the samples examined.

(3) (a) Stuzhin, P. A.; Bauer, E. M.; Ercolani, C. *Inorg. Chem.* **1998**, *37*, 1533. (b) Bauer, E. M.; Cardarilli, D.; Ercolani, C.; Stuzhin, P. A.; Russo, U. *Inorg. Chem.* **1999**, *38*, 6114. (c) Bauer, E. M.; Ercolani, C.; Galli, P.; Popkova, I. A.; Stuzhin, P. A. *J. Porphyrins Phthalocyanines* **1999**, *3*, 371. (d) Angeloni, S.; Bauer, E. M.; Ercolani, C.; Popkova, I. A.; Stuzhin, P. A. *J. Porphyrins Phthalocyanines* **2001**, *5*, 881. (e) Donzello, M. P.; Ercolani, C.; Stuzhin, P. A.; Chiesi-Villa, A.; Rizzoli, C. *Eur. J. Inorg. Chem.* **1999**, 2075.

(4) (a) Stuzhin, P. A.; Ercolani, C. *The Porphyrin Handbook*; Kadish, K. M.; Smith, K. M.; Guilard, R., Eds.; Academic Press: New York, 2003; Vol. 15, Chapter 101, pp 263−364. (b) Kudrevich, S. V.; van Lier, J. E. *Coord. Chem. Rev.* **1996**, *156*, 163.

(5) Fisher, M. S.; Templeton; D. H.; Zalkin, A.; Calvin, M. *J. Am. Chem. Soc.* **1971**, *93*, 2622.

(6) Velasquez, S. V.; Fox, G. A.; Broderick, W. E.; Andersen, K. A.; Anderson, O. P.; Barrett, A. G. M.; Hoffman, B. M. *J. Am. Chem. Soc.* **1992**, *114*, 7416.

(7) Matzumoto, S.; Endo, A.; Mizuguchi, J. *Z. Krystallogr.* **2000**, *215*, 182.

(8) Baum, S. M.; Tra banco, A. A.; Montalban, A. G.; Micallef, A. S.; Zhong, C.; Meunier, H. G.; Suhling, K.; Phillips, D.; White, A. J. P.; Williams, D. J.; Barrett, A. G. M.; Hoffman, B. M. *J. Org. Chem.* **2003**, *68*, 1665.

Table 1. Room Temperature Magnetic Moment and Low Temperature (80 K) EPR Data of Solvated [Py_8TPyzPzM] Complexes and Other Porphyrazine Analogues

complex[a]	diam corr $\times 10^6$ (cgsu)	μ_{eff}[b] (μ_B)	$g_{\|}$	$g_{\perp}$	$A_{\|}^M$ (G)	$A_{\perp}^M$ (G)	$A_{\|}^N$ (G)	ref
[Py_8TPyzPzCu]·$5H_2O$[c]	−668	1.91	2.173	2.056	205	16	16	TP[f]
[TTDPzCu]·$2H_2O$		1.93	2.190	2.064	203	16	16	3b[g]
[TSeDPzCu]·$3H_2O$·CH_3COOH		2.29	2.178	2.056	204	17	13	3d[g]
[Ph_8DzPzCu]·$5H_2O$[d]		2.04	2.149	2.046	220	18	16	2a
[Py_8TPyzPzCo]·$8H_2O$[d]	−707	3.05	2.006	2.21	96.4	31		TP
[Ph_8DzPzCo]·$8H_2O$[d]		3.05	2.181	2.611	238	91		2a
[Py_8TPyzPzMn]·$3H_2O$[e]	−643	5.46						TP

[a] EPR spectral data of the complexes listed were all obtained from samples magnetically diluted in the corresponding Zn^{II} complex matrixes (water molecules not necessarily corresponding to the formula given in the table). [b] $\mu_{eff} = 2.84 \times (\chi_M' \cdot T)^{1/2}$. [c] Prepared from pyridine. [d] Prepared from DMSO. [e] Prepared from pyridine, desolvated by heating under vacuum, and then exposed to the air. [f] TP: this paper. [g] EPR data taken at room temperature.

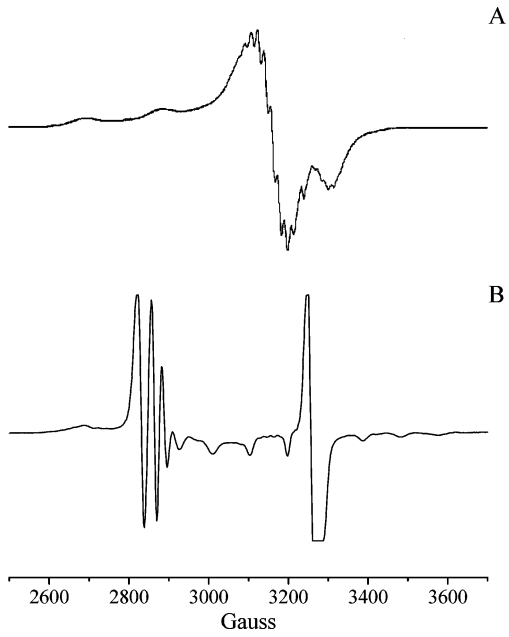

Figure 2. Low temperature (77 K) EPR spectra of [Py_8TPyzPzCu] (A) and [Py_8TPyzPzCo] (B) magnetically diluted in their corresponding Zn^{II} matrix. In spectrum B, the peak present at ca. 3250 G is due to a π-radical impurity found to be present also in the parallel sample of the pure Zn^{II} complex.

The room temperature magnetic moment of the Cu^{II} complex, 1.91 μ_B, is close to values found for similar species (Table 1) and indicates the presence of one unpaired electron, as expected. The EPR spectrum of a solid sample prepared by diluting the Cu^{II} complex in the respective Zn^{II} matrix shows hyperfine and superhyperfine structure (Figure 2A). The measured g and A values, in keeping with other data (Table 1), certainly prove charge delocalization of the unpaired electron within the CuN_4 central moiety. As to the Co^{II} complex, its room temperature μ_{eff} value (3.05 μ_B), although significantly higher than that expected for the spin-only value (1.73 μ_B), suggests a low-spin structure, in line with values found for the diazepinoporphyrazine complex [Ph_8DzPzCo]·$8H_2O$ (prepared in pyridine:[2a] 3.05 μ_B; Table 1), for the phthalocyanine complex [PcCo] (2.69 μ_B),[10] and for other low-spin square planar Co^{II} complexes (μ_{eff} = 2.2−2.9 μ_B).[11] The EPR spectrum of [Py_8TPyzPzCo] also shows hyperfine and superhyperfine structure (Figure 2B) confirming the low-spin electronic state and electron delocalization in the CoN_4 porphyrazine core.

The μ_{eff} value of the Mn^{II} complex, in the form of a trishydrate, i.e., [Py_8TPyzPzMn]·$3H_2O$, is 5.46 μ_B. This is a little lower than the calculated spin-only value for five unpaired electrons (d^5, 5.92 μ_B) and the experimental values measured for the Mn^{II} tetrakis[(1,2,5-thia(seleno)diazolo]porphyrazines, [TTDPzMn] (5.98 μ_B)[3b] and [TSeDPzMn] (5.78 μ_B),[3d] but it is considerably higher than for the Mn^{II}−phthalocyanine, i.e., [PcMn] (4.34 μ_B, $S = {}^3/_2$).[10] It is also higher than what has recently been reported for the "diazepinoporphyrazine" Mn^{II} complex [Ph_8DzPzMn]·$5H_2O$ (5.10 μ_B).[2a] The observed value for [Py_8TPyzPzMn]·$3H_2O$ suggests a high-spin configuration, probably partially quenched by some form of interunit spin−spin magnetic interaction. We failed to obtain reliable information from EPR spectra for the Mn species.

Solution Studies. UV−Vis Spectra. The UV−vis spectral behavior of the [Py_8TPyzPzM] complexes (M = $Mg^{II}(H_2O)$, Mn^{II}, Co^{II}, Cu^{II}, Zn^{II}) was studied in three types of solvents, i.e., nondonor solvents ($CHCl_3$, CH_2Cl_2), weakly basic solvents (pyridine, DMSO), and an acidic solvent (CH_3COOH). The complexes show sufficient solubility in pyridine, DMSO, and CH_3COOH (ca. 10^{-4}−10^{-5} M). A markedly lower solubility is generally found in CH_2Cl_2 or $CHCl_3$, the only exceptions being for the Cu^{II} and Zn^{II} complexes where the solubility in the two nondonor solvents is comparable to what is seen in the more polar solvents.

Molecular aggregation, i.e., intermolecular association, very likely pre-existing in some form in the solid state, is often observed to be present immediately after dissolution of the complexes in the different solvents, with its occurrence and duration depending upon the nature of the metal complex and the medium used. If it occurs, the solutions obtained, after normal centrifugation of the undissolved ground material, show initially some turbidity associated with the formation of a "colloidal" suspension, similar to what was observed for the unmetalated macrocycle.[1] The UV−vis spectral changes which occur as a function of time indicate in all cases a one-way process, ending with formation of monomeric macrocyclic units. Figure 3 shows the spectral behavior of the Cu^{II} complex in pyridine as a representative example (quite similar spectral evolutions are observed in

(9) Figgis, B. M.; Lewis, J. In *Modern Coordination Chemistry*; Lewis, J., Wilkins, R. G., Eds.; Interscience Publishers Inc.: New York, 1960; pp 400−454.
(10) Lever, A. B. P. *J. Chem. Soc.* **1965**, 1821.
(11) Figgis, B. M.; Nyholm, R. S. *J. Chem. Soc.* **1954**, 12.

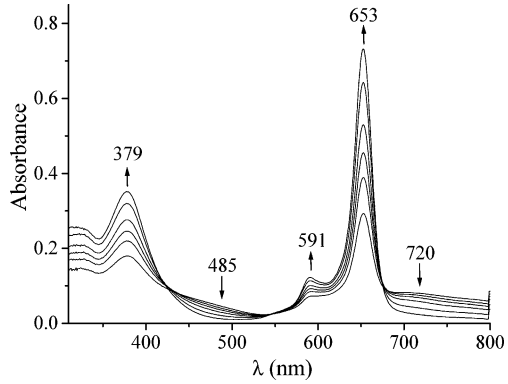

Figure 3. UV−vis spectral changes of [Py_8TPyzPzCu] in pyridine solution as a function of time.

DMSO, DMF, CH_3CN, CH_2Cl_2, CH_3COOH; see Figure S1 in Supporting Information). These spectra are characterized initially by the presence of a low-intensity absorption, at ca. 720 nm (as is also seen for the free-base ligand). This broad band progressively decreases in intensity with time after solution preparation and finally disappears, while concomitantly the Q band increases and reaches its maximum intensity (peak at 653 nm for the Cu^{II} complex, Figure 3; final spectrum after ca. 30 min). The final spectrum (clear solution) is as expected for a normal porphyrazine macrocycle of D_{4h} symmetry, since it shows an unsplit sharp Q band in the 600−700 nm region, plus an absorption envelope in the Soret region.[12] The presence of well-defined isosbestic points indicates the absence of spectrally detectable intermediates as the compound dissolves. These findings strictly parallel the behavior shown by the corresponding unmetalated macrocycle in different solvents,[1] with the exception of expected differences due to the symmetry of [Py_8TPyzPzH$_2$] (D_{2h}), which has a split Q band, and the [Py_8TPyzPzM] complexes (D_{4h}), which have unsplit Q bands.[12]

Table 2 summarizes the quantitative UV−vis spectral data taken in pyridine solution for the monomeric form of the examined complexes. Qualitative spectra in the other solvents are reported in Table S1 in Supporting Information. For each individual species dissolved in a specific solvent, peak positions were recorded for the final spectrum whenever there were spectral changes with time.

The monomeric [Py_8TPyzPzM] complexes, with the exception of the Mn^{II} derivative (see below), all have fairly similar spectral features in the different solvents and closely resemble what is shown in Figure 3 for the final spectrum of the Cu^{II} complex in terms of relative intensities of the B band envelope and Q band absorption. Only a slight dependence of peak position is observed for the [Py_8TPyzPzM] complexes as a function of the solvent, the largest red-shift of the Q band being systematically observed in solutions of glacial CH_3COOH, probably as a result of an interaction between the acid and the pyrazine and pyridine N atoms. A splitting of the Q band is observed for the Zn complex in both $CHCl_3$ and CH_2Cl_2, whereas no splitting is seen for the compound in the more polar pyridine, DMSO, or CH_3COOH. This splitting is probably due to some form of excitonic coupling due to molecular association and has been reported for zinc, copper, and vanadyl tetraoctadecylsulfonamido-phthalocyanines.[13] It is noteworthy that the Mg^{II} porphyrazine complex, for which the initial spectrum in CH_3COOH indicates that it is monomeric immediately upon dissolution, shows spectral changes indicative of progressive demetalation and formation of the free-base ligand (D_{2h} symmetry, split Q band[1]).

The spectrum of [Py_8TPyzPzMn] in pyridine is given in Figure 4. There is a broad intense envelope in the region 480−580 nm, with peaks at 532 and 564 nm, very likely responsible for the purple-violet color of the solution. In addition, there is a very intense B band with maximum at 346 nm with a shoulder at ca. 400 nm and two lower intensity peaks at 644 nm (Q band) and 783 nm. The central broad envelope and the peak at 783 nm as well are almost certainly due to some type of Mn → L(ligand) or L → Mn charge transfer (CT). The lower relative intensity of the Q band is not unexpected in the presence of closely lying charge-transfer absorptions in the 500 nm region, as described elsewhere.[14a] On the basis of the observed tendency shown by [Py_8TPyzPzMn], and by [Py_8TPyzPzCo] as well (see above), to retain pyridine in the solid state when prepared in this solvent, it seems plausible that [Py_8TPyzPzMn], high-spin in the solid state after complete elimination of pyridine, might coordinate with the pyridine solvent in solution and change its high-spin state to a low-spin configuration after formation, supposedly, of a six-coordinate pyridine adduct, [Py_8TPyzPzMn(py)$_2$].

In an attempt to relate the [Py_8TPyzPzMn] complex to similar species described in the literature, it should be noted that, to our knowledge, there are almost no examples of Mn^{II} porphyrazine analogues which can be used for comparison,[4] with the only exception being Mn^{II} phthalocyanine, [PcMn],[15] and some of its substituted analogues.[16] The solution spectral behavior of [PcMn] is fairly intriguing and found to depend on a number of experimental conditions, i.e., the nature and purity of the solvent and the presence of water and/or oxygen. Nevertheless, if [PcMn] is treated with *N*-methylimidazole (*N*-MeIm), a low-spin bis-adduct is formed, i.e., [PcMn(*N*-MeIm)$_2$].[17] This species has a spectrum in DMA which shares similarities to that of the [Py_8TPyzPzMn]

(12) (a) Stillman, M. J. In *Phthalocyanines: Properties and Applications*; Leznoff, C. C., Lever, A. B. P., Eds.; VCH Publishers: New York, 1989; Vol. 1, pp 133−289. (b) Mack, J.; Stillman, M. J. In *The Porphyrin Handbook*; Kadish, K. M., Smith, K. M., Guilard, R., Eds.; Academic Press: New York, 2003; Vol. 16, pp 43−116. (c) Gouterman, M. In *The Porphyrins*; Dolphin, D., Ed.; Academic Press: New York, 1978; Vol. III and references therein.

(13) Monahan, A. R.; Brado, J. A.; DeLuca, A. F. *J. Phys. Chem.* **1972**, *76*, 1994.

(14) (a) Stillman, M. J. In *Phthalocyanines Properties and Applications*; Leznoff, C. C., Lever, A. B. P., Eds.; VCH Publishers Inc.: New York, 1989; Vol. 1, p 149. (b) Stillman, M. J.; Thomson, A. J. *J. Chem. Soc., Faraday Trans. 2* **1974**, *70*, 790.

(15) Minor, P. C.; Lever, A. B. P. *Inorg. Chem.* **1983**, *22*, 826 and references therein.

(16) Dolotova, O. V.; Bundina, N. I.; Kaliya, O. L.; Lukyanets, E. A. *J. Porphyrins Phthalocyanines* **1997**, 355.

(17) Wilshire, J. P.; Lever, A. B. P. Unpublished data. See: Stillman, M. J. In *Phthalocyanines Properties and Applications*; Leznoff, C. C., Lever, A. B. P., Eds.; VCH Publishers Inc.: New York, 1989; Vol. 1, pp 204−205.

Table 2. UV−Vis Spectral Data (λ, nm (log ϵ)) for the Hydrated Species [$Py_8TPyzPzM$] (M = $Mg(H_2O)$, Cu, Zn, Mn, Co) in Pyridine

M	Soret region		CT region		Q-band region[a]			
Mg[b]	375 (5.23)				596 (4.65)	631 (sh)	*658* (5.54)	
Cu[c]	379 (4.64)				591 (4.18)		*653* (4.93)	
Zn[c,d]	378 (4.90)				598 (4.31)	630 (sh)	*658* (5.18)	
Mn[b,e]	346 (4.71)	401 (sh)	532 (4.54)	564 (4.54)			*644* (4.28)	783 (3.98)
Co[b,e]	364 (5.01)	441 (4.40)		575 (sh)			*635* (4.94)	

[a] The main absorption in the Q-band region is given in italics. [b] From DMSO. [c] From pyridine. [d] Final spectrum after a minimum of 2 h. [e] Solutions immediately clear after dissolution.

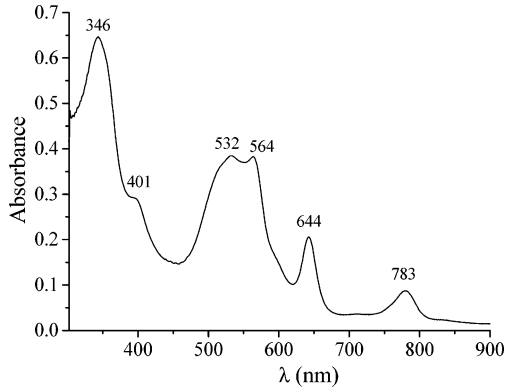

Figure 4. UV−vis spectrum of [$Py_8TPyzPzMn$] in pyridine.

species in pyridine; i.e., after complexation by the N-base, the Soret and Q bands are accompanied by new absorptions in the spectral window 400−550 nm (peaks at 477 and 544 nm) with additional peaks on the red side of the Q band. However, despite these data, whether the CT band observed for [$Py_8TPyzPzMn$] in pyridine is of the type Mn → L or L → Mn remains uncertain on the basis of UV−vis spectral data alone.

Electrochemical and EPR Measurements. Electrochemical and spectroelectrochemical measurements were conducted on all metal derivatives in pyridine, and for the Cu^{II} and Zn^{II} complexes also in CH_2Cl_2, taking advantage of the solubility of these two complexes in this solvent. Figure 5 shows the cyclic voltammograms obtained at a scan rate of 100 mV/s. Half-wave potential values ($E_{1/2}$, V vs SCE) are listed in Table 3 together with those of the "diazepinoporphyrazine" and the phthalocyanine analogues for comparison. As is also the case for the unmetalated species, [$Py_8TPyzPzH_2$] (see for discussion ref 1), four reversible one-electron reductions are observed for all of the metal complexes. The $E_{1/2}$ values are similar for the Cu^{II} and Zn^{II} derivatives in the two solvents (pyridine and CH_2Cl_2) which indicates that the processes are not significantly solvent dependent.

Extremely well-defined cyclic voltammograms are also obtained in a thin-layer cell, and this is illustrated in Figure 6 which shows the resulting current voltage curves for the Cu^{II}, Zn^{II}, Mn^{II}, and Co^{II} derivatives. The first two compounds contain electroinactive metal ions while the Mn^{II} and Co^{II} porphyrazines can be oxidized to their respective M(III) oxidation state. Reduction at the Co^{II} center can also occur and is well-documented in the literature.

Several points are of interest with respect to the data in Figure 6, the most notable of which is the $E_{1/2}$ value of the third reduction process which occurs at virtually identical potentials, independent of the type of the central metal ion. The overall sequence of redox processes for the Cu^{II}, Zn^{II}, and Mg^{II} complexes is given by eqs 1−4, and this is also proposed in the case of the Mn^{II} species.

$$[Py_8TPyzPzM] + e^- \rightleftarrows [Py_8TPyzPzM]^- \quad (1)$$

$$[Py_8TPyzPzM]^- + e^- \rightleftarrows [Py_8TPyzPzM]^{2-} \quad (2)$$

$$[Py_8TPyzPzM]^{2-} + e^- \rightleftarrows [Py_8TPyzPzM]^{3-} \quad (3)$$

$$[Py_8TPyzPzM]^{3-} + e^- \rightleftarrows [Py_8TPyzPzM]^{4-} \quad (4)$$

A different sequence of steps, which will be discussed in more detail below, is proposed for reduction of [$Py_8TPyzPzCo^{II}$]. The first two steps are suggested to occur as shown in eqs 5 and 6, and the next two processes are as shown in eqs 3 and 4.

$$[Py_8TPyzPzCo^{II}] + e^- \rightleftarrows [Py_8TPyzPzCo^{I}]^- \quad (5)$$

$$[Py_8TPyzPzCo^{I}]^- + e^- \rightleftarrows [Py_8TPyzPzCo^{II}]^{2-} \quad (6)$$

With specific reference to eq 6, it should be noted that the conversion of a Co(I) porphyrazine to a Co(II) dianion upon reduction by one electron is not without precedent in the literature and has been demonstrated to occur in the case of an easily reducible porphyrin.[18] Evidence for this assignment is given in part by spectroelectrochemical data presented in a later section and in part by the half-wave potential of −1.36 V for the third reduction which matches, within experimental error, the $E_{1/2}$ values for the same processes of the Cu(II) and Zn(II) derivatives (see Figure 6). In this respect, it can be noted that the $E_{1/2}$ values in Figure 6 differ slightly from those in Figure 5 and Table 3, and this is attributed to the different concentrations of supporting electrolyte between the two experimental conditions (0.2 M in thin-layer CV and 0.1 M under "routine" cyclic voltammetric conditions).

Finally, it should be pointed out that the absolute potential separation between any two sets of half wave potentials (Δ_{1-2}, Δ_{2-3}, and Δ_{3-4}) differs somewhat from what is observed for the free-base [$Py_8TPyzPzH_2$] macrocycle under the same experimental conditions.[1] For example, in the case of the free-base macrocycle, these three separations are 0.35, 0.81, and 0.34 V in CH_2Cl_2,[1] and this can be compared to an average separation of 0.37, 0.68, and 0.28 V for the Zn^{II} and Cu^{II} derivatives, under the same experimental condi-

(18) Araullo-McAdams, C.; Kadish, K. M. *Inorg. Chem.* **1990**, *29*, 2749.

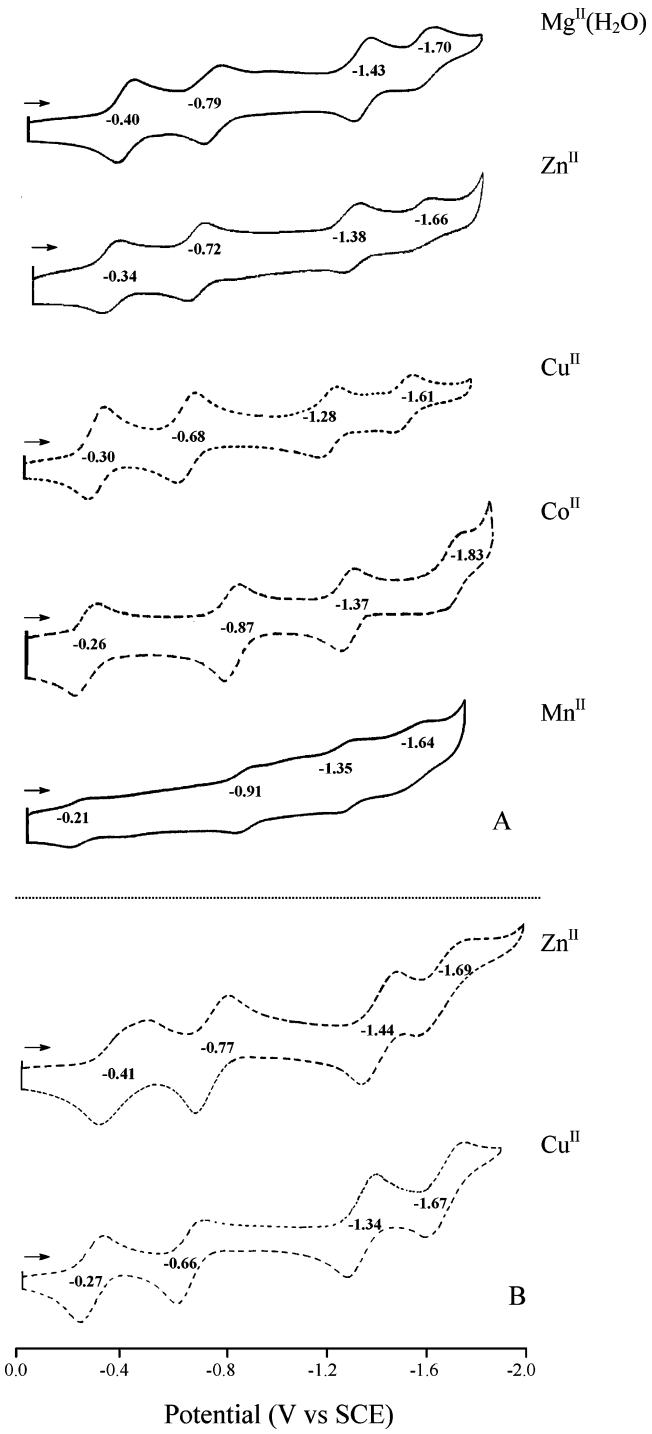

Figure 5. Cyclic voltammograms, with added $E_{1/2}$ values, of [Py_8TPyzPzM] complexes in pyridine (A) and CH_2Cl_2 (B); 0.1 M TBAP, scan rate 100 mV/s (— first scan; - - - second scan).

tions (see Table 3). The Δ_{1-2}, Δ_{2-3}, and Δ_{3-4} values for [Py_8PyzPzMn] are 0.70, 0.44, and 0.29 V in pyridine (see Figure 5) while in the case of [Py_8TPyzPzCo] the three separations are 0.61, 0.50, and 0.46 V. Most notable, however, is the fact that the third reduction of [Py_8PyzPzM] varies little with the metal ion as shown in the thin-layer voltammograms of Figure 6 and already mentioned above.

Details of the spectroelectrochemical behavior and EPR data for the [Py_8TPyzPzM] complexes are given below and discussed in the following order: $Mg^{II}(H_2O)$, Zn^{II}, Cu^{II}, Co^{II}, Mn^{II}.

M = Mg^{II} and Zn^{II}. Figure 7 depicts the spectral changes of the Mg^{II} complex in pyridine during the first and second thin-layer reductions (−0.40 and −0.79 V vs SCE, respectively). The first reduction (Figure 7A) is accompanied by a complete disappearance of the Q band (this is also observed for the free-base ligand), a decrease in intensity, broadening, and shift (375 → 317 nm) of the B band envelope in the Soret region, and the appearance of new weak absorptions at 454, 566, and 704 nm. The second reduction (Figure 7B) mainly results in an increase in intensity of the 566 nm band accompanied by only small changes in the other regions of the spectrum. A reversibility of the two redox processes is observed by the stepwise reoxidation which leads to full regeneration of the spectrum of the initial neutral species. No evidence for detectable aggregation is observed in the overall evolution. The third and fourth reduction steps ($E_{1/2}$ = −1.43 and −1.70 V vs SCE) are also accompanied by reversible spectral changes (not shown), which mainly consist of an increase in intensity of the B band at 325 nm and a complete disappearance of the 566 nm absorption.

The Zn^{II} complex shows an analogous spectroelectrochemical pattern in pyridine, although some aggregated species are present. Since Mg^{II} and Zn^{II} are closed shell central ions and both are redox inactive, all reductions are obviously ligand-centered, with the added electrons accommodated in the ligand e_g orbital level.[12] As expected, the EPR spectrum of the singly reduced Zn^{II} species shows a narrow peak (ΔH = 21 G, g = 2.001; 223 K), diagnostic for formation of the ligand π-radical anion [Py_8TPyzPzZn]$^-$.

M = Cu^{II}. Consistent with the cyclic voltammograms in Figures 5 and 6, reversibile one-electron reduction processes are observed for the Cu^{II} complex in pyridine and CH_2Cl_2 (see Table 3) with $E_{1/2}$ values a little less negative than those of the Mg^{II} and Zn^{II} complexes. Thus, the stepwise reduction is favored in the sequence Mg^{II} < Zn^{II} < Cu^{II} for each distinct step of reduction. From the data of Table 3, it can also be seen that the difference in the $\Delta E_{1/2}$ values, i.e., Δ_{1-2}, Δ_{2-3}, and Δ_{3-4}, are very similar for the three complexes. This similarity indicates that the stepwise electron uptake by Cu^{II} complex, as is also the case for the Mg^{II} and Zn^{II} complexes, is exclusively confined to the ligand macrocyclic unit with no involvement of the central metal ion. The fully reversible spectral changes associated with the redox processes for the Cu^{II} complex quite closely resemble what is observed for the Mg^{II} and Zn^{II} macrocycles.

M = Co^{II} and Mn^{II}. The first one-electron reduction of [Py_8TPyzPzCo] in pyridine (Figure 5) occurs at an $E_{1/2}$ value slightly less negative than the first reduction processes of the Mg^{II}, Zn^{II}, and Cu^{II} species examined above (Table 3), whereas the second and fourth reductions occur at more negative values by ca. 0.2 V, the third one more or less coinciding with the value of the Zn^{II} complex.

Combined EPR and spectroelectrochemical measurements for [Py_8TPyzPzCo] in pyridine provide substantial information on the site of the first and second one-electron reduction. The EPR spectra at 77 K of [Py_8TPyzPzCo] and its

Table 3. Half-Wave Potentials ($E_{1/2}$, V vs SCE) of the Hydrated Species [Py_8TPyzPzM] (M = Mg, Zn, Cu, Co, Mn, 2H) and Analogues in Pyridine, CH_2Cl_2, or DMF, 0.1 M TBAP (Scan Rate = 100 mV/s)

		reduction					$\Delta E_{1/2}$				
compd	solvent	first	second	third	fourth	fifth	Δ_{1-2}	Δ_{2-3}	Δ_{3-4}	Δ_{4-5}	ref[a]
[Py_8TPyzPzMg(H_2O)]	py	−0.40	−0.79	−1.43	−1.70		0.39	0.64	0.27		TP
[Py_8TPyzPzZn]	py	−0.34	−0.72	−1.38	−1.66	−1.83	0.38	0.66	0.28	0.17	TP
[Py_8TPyzPzCu]	py	−0.30	−0.68	−1.28	−1.61		0.38	0.61	0.33		TP
[Py_8TPyzPzCo]	py	−0.26	−0.87	−1.37	−1.83		0.61	0.50	0.46		TP
[Py_8TPyzPzMn]	py	−0.21	−0.91	−1.35	−1.64		0.70	0.44	0.29		TP
[Py_8TPyzPzZn]	CH_2Cl_2	−0.41	−0.77	−1.44	−1.69		0.36	0.67	0.25		TP
[Py_8TPyzPzCu]	CH_2Cl_2	−0.27	−0.66	−1.34	−1.67		0.39	0.68	0.33		TP
[Py_8TPyzPzH_2]	CH_2Cl_2	−0.15	−0.50	−1.31	−1.65		0.35	0.81	0.34		TP
[Ph_8DzPzZn]	py	−0.72	−1.04	−1.33	−1.49	−1.72	0.32	0.29	0.16	0.13	2a
[Ph_8DzPzCu]	py	−0.56	−0.79	−1.10	−1.30	−1.48	0.23	0.31	0.20	0.18	2a
[Ph_8DzPzMn]	py	−0.52	−0.88	−1.22	−1.51		0.36	0.34	0.29		2a
[Ph_8DzPzCo]	py	−0.49	−0.73	−1.05	−1.40	−1.68	0.24	0.32	0.35	0.28	2a
[Ph_8DzPzH_2]	CH_2Cl_2	−0.42	−0.66	−1.02	−1.15	−1.34	0.24	0.34	0.13	0.19	2a
[PcMg]	DMF	−0.91	−1.39	−2.14	−2.58		0.48	0.75	0.44		20a
[PcZn]	DMF	−0.89	−1.33	−2.06	−2.68		0.44	0.73	0.62		20a
[PcCu]	DMF	−0.84	−1.18	−2.01	−2.28		0.34	0.83	0.27		20a
[PcCo]	DMF	−0.37	−1.40	−1.80	−2.08	−2.46	1.03	0.40	0.28	0.38	20a
[PcH_2]	DMF	−0.66	−1.06	−1.93	−2.23		0.40	0.87	0.30		20a

[a] TP = this paper.

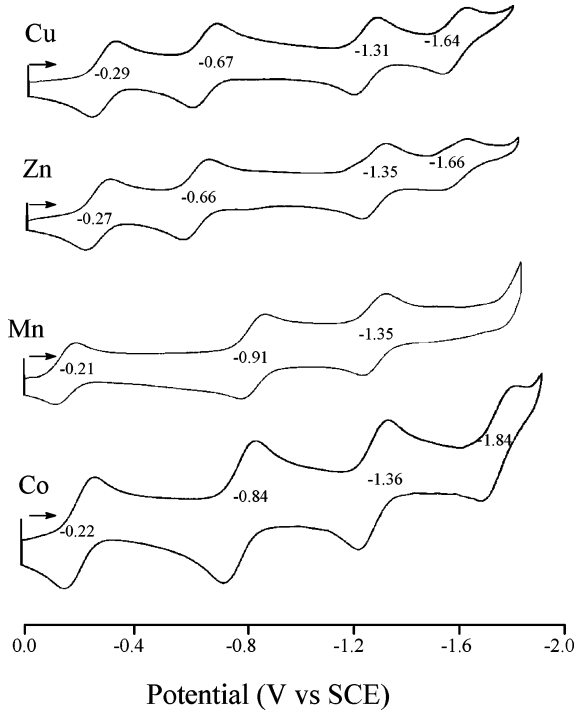

Figure 6. Cyclic voltammograms obtained in a thin-layer cell for the species [Py_8TPyzPzM], where M = Cu, Zn, Mn, or Co, in pyridine containing 0.2 M TBAP at a scan rate of 10 mV/s.

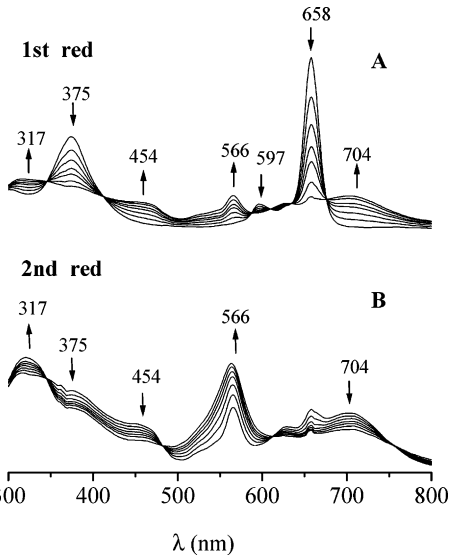

Figure 7. UV−vis spectral changes in pyridine containing 0.2 M TBAP during controlled potentials electrolysis of [Py_8TPyzPzMg(H_2O)] at (A) −0.55 V (first reduction) and (B) −0.85 V (second reduction).

corresponding mononegatively charged ion are shown in Figure 8. The spectrum of [Py_8TPyzPzCo] (Figure 8A), indicative of the presence of Co^{II} in a tetragonal environment ($g_{\|} = 2.01$; $g_{\perp} = 2.16$), is changed, after the first one-electron reduction, into the spectrum of Figure 8B. This spectrum shows only a weak residual signal likely to be due to traces of some unknown impurity. It also shows the complete absence of the previous Co^{II} resonance peak and of a narrow intense peak at $g \cong 2$ attributable to the formation of a ligand-centered π-anion radical. Hence, these findings appear to indicate a "metal-centered" reduction with formation of Co^{I} (d^8, low-spin, diamagnetic) in the negatively charged ion [Py_8TPyzPzCo^{I}]$^-$.

Parallel spectroelectrochemical measurements on [Py_8TPyzPzCo] seem to further support the EPR findings. Figure 9A shows that [Py_8TPyzPzCo] has a "normal" UV−vis spectrum in pyridine with a Q band at 635 nm and an intense peak in the Soret region with maximum at 362 nm and a shoulder at 441 nm.

Significant spectral changes are produced upon the one-electron reduction to give [Py_8TPyzPzCo^{I}]$^-$. The spectrum of the anion shows an intense broad flat peak centered at ca. 545 nm, with the Q band being considerably red-shifted (695 nm) and appearing at relatively lower intensity and the Soret band moved to higher energy (335 nm) with a decreased intensity. Since [Py_8TPyzPzCo^{I}]$^-$ has no unpaired electrons and hence has no radical character, the broad

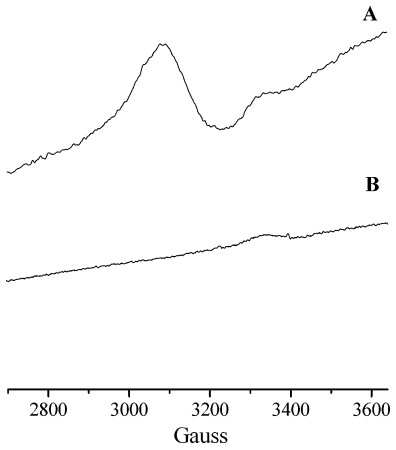

Figure 8. Low temperature (77 K) EPR spectra in pyridine containing 0.2 M TBAP of (A) the neutral complex [Py_8TPyzPzCo] and (B) the mononegatively charged anion [Py_8TPyzPzCoI]$^-$ obtained after first reduction at controlled potential (−0.50 V).

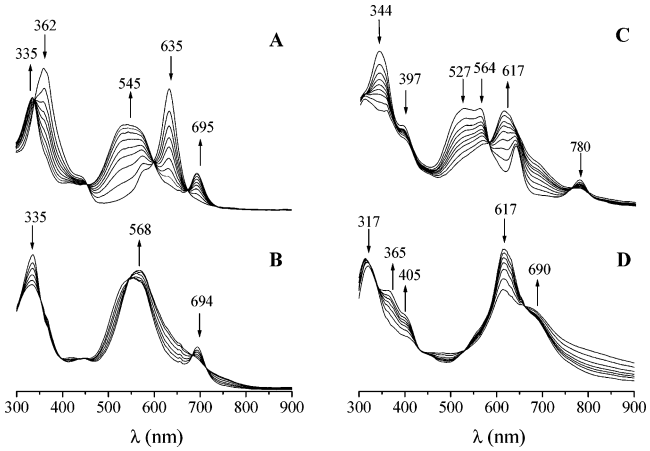

Figure 9. UV−vis spectral changes in pyridine containing 0.2 M TBAP during controlled potential electrolysis of [Py_8TPyzPzCo] at (A) −0.50 V (first reduction) and (B) −1.10 V (second reduction), and of [Py_8TPyzPzMn] at (C) −0.50 V (first reduction) and (D) −1.20 V (second reduction).

absorption observed at 545 nm must be assigned as a charge-transfer band. Quite remarkably, the spectrum of this −1 charged species closely approaches that of its phthalocyanine analogue [PcCo^I]$^-$ as obtained after the one-electron reduction of [PcCo] in DMSO[14b] (broad intense band envelope in the 450−500 nm region, Q band red-shifted to 700 nm) and in pyridine (spectrum with bands at 311, 426, 467, 604, and 704 nm).[19]

Similar features have been reported for the spectrum of [PcCo^I]$^-$ in THF[20b] which has a CT absorption band at 460 nm. All authors[14b,19,20b] have agreed in assigning the CT absorption as an M → L charge transfer, a type of assignment also proposed in the current work for the broad absorption of [Py_8TPyzPzCo^I]$^-$ centered at ca. 545 nm. Interestingly, the spectrum of this anion is also strongly reminiscent of that previously discussed for the neutral Mn^{II} species (see Figure 4).

The second one-electron uptake by [Py_8TPyzPzCo^I]$^-$ brings back Co^I to Co^{II} and forms the dianion [Py_8TPyzPzCo^{II}]$^{2-}$, in which the two added electrons are now residing in the ligand framework in a spin-paired state. This proposed mechanism is discussed earlier (see eq 6). It differs for what is seen in the case of [PcCo] where the first two reductions produce [PcCo^I]$^-$ and [PcCo^I]$^{2-}$, the latter species being one which has one added electron located on the metal center and the other on the phthalocyanine ring.[20b]

The UV−vis spectral changes in going from [Py_8TPyzPzCo^I]$^-$ to [Py_8TPyzPzCo^{II}]$^{2-}$ are also shown in Figure 9. A new absorption appears on the second reduction with a maximum at 568 nm at the expense of the CT band at 545 nm, whereas the Soret band (335 nm) and Q band (694 nm) slightly decrease in intensity. Noteworthy, the 568 nm band is certainly not CT in nature. In fact, a similar absorption systematically appears at ca. 560−565 nm, steeply gaining in intensity upon the second reduction in the spectra of the Mg^{II} (Figure 7, 566 nm), Zn^{II} (565 nm), and Cu^{II} complexes (561 nm). Moreover, for the same complexes, the spectra reproducibly show a strong decrease in intensity upon the third reduction and a loss of all spectral details after the fourth reduction. The electrochemical removal of two electrons from [Py_8TPyzPzCo^{II}]$^{2-}$, i.e., reoxidation to the neutral species, leads to a full recovery of the initial EPR and UV−vis spectra.

As to the Mn^{II} complex, Figure 9 shows the UV−vis spectral changes which take place during formation of [Py_8TPyzPzMn]$^-$ and [Py_8TPyzPzMn]$^{2-}$ in the thin-layer cell. The broad central CT envelope with maxima at 527 and 564 nm (already discussed above) disappears almost completely, while the Q band, blue-shifted (644 → 617 nm), gains in intensity and the B band envelope broadens, markedly decreasing in intensity similar to the absorption at 780 nm. As to this first reduction step, we have at present no useful EPR data to establish whether this reduction is metal- or ring-centered. Only small and not significant spectral changes are observed during the second reduction, the only change worthy of notice being a decrease in intensity of the Q band.

As seen in Table 3, the first reduction of the [Py_8TPyzPzM] complexes is increasingly favored (more positive $E_{1/2}$) in the sequence Mg^{II}(H$_2$O) < Zn^{II} < Cu^{II} < Co^{II} < Mn^{II}. Thus, the Mn^{II} complex is the most easily reduced among the metal derivatives. If account is taken that the Zn^{II} and Cu^{II} complexes exhibit $E_{1/2}$ values in CH_2Cl_2 similar to what is observed in pyridine, and the single metals, i.e., Zn^{II} or Cu^{II}, have $E_{1/2}$ values practically coincident in the two solvents, then it is easily concluded that the $E_{1/2}$ value of the first reduction measured for the unmetalated macrocycle qualifies this latter as the most easily reduced among all the series explored, a feature which is maintained also for the 2nd, 3rd, and 4th reduction processes.

(19) Day, P.; Hill, H. A. O.; Price, M. G. *J. Chem. Soc. A* **1968**, 90.
(20) (a) Clack, D. W.; Hush, N. S.; Woolsey, I. S. *Inorg. Chim. Acta* **1976**, *19*, 129. (b) Clack, D. W.; Yandle, J. R. *Inorg. Chem.* **1972**, *11*, 1738.
(21) (a) Shirk, J. S.; Pong, R. G. S.; Bartoli, F. J.; Snow, A. W. *Appl. Phys. Lett.* **1993**, *63*, 1880. (b) Perry, J. W.; Mansour, K.; Lee, I. Y. S.; Wu, X. L.; Bedworth, P. V.; Chen, C.-T.; Ng, D.; Marder, S. R.; Miles, P. *Science* **1996**, *273*, 1533. (c) Shirk, J. S.; Pong, R. G. S.; Flom, S. R.; Heckmann, H.; Hanack, M. *J. Phys. Chem. A* **2000**, *104*, 1438. (d) Blau, W.; Byrne, H.; Dennis, W. M.; Kelly, J. M. *Opt. Commun.* **1985**, *56*, 25. (e) Vagin, S.; Barthel, M.; Dini, D.; Hanack, M. *Inorg. Chem.* **2003**, *42*, 2683.

Table 3 also lists half-wave potentials for the corresponding reductions of a series of diazepinoporphyrazine macrocycles[2a] as well as $E_{1/2}$ values for the peripherally unsubstituted phthalocyanine analogues.[17] From a comparison of the data, it can be said that the reduction potentials for the present [Py_8TPyzPzM] species occur systematically at less negative potentials than for the other two series of compounds. This means that the electron-withdrawing effect of the annulated pyrazine rings, highly influenced by the presence of the externally appended pyridine rings in the pyridinopyrazinoporphyrazine species, remarkably facilitate the addition of electrons and redistribution of the negative charge on the entire macrocyclic entity. This aspect is also emphasized by the reversibility exhibited by the four successive one-electron reductions, clearly indicating the stability of the different negatively charged species that are formed.

Nonlinear Optical Transmission Measurements. Multiphoton absorption based on a reverse saturable absorption (RSA) mechanism involving triplet excited states is known to be active for structures such as phthalocyanines, porphyrines, and porphyrazines.[21] Porphyrazines have molecular structural features with important electronic differences from their parent phthalocyanine and porphyrins analogues, and this makes them interesting materials for nonlinear optical studies.[2,22] The nonlinear transmission measurements on some of the present macrocycles [Py_8TPyzPzM] (M = $2H^I$, $Mg^{II}(H_2O)$, Cu^{II}, Zn^{II}) were obtained in an open aperture configuration (collection solid angle: 0.1 sterad) to determine the multiphoton absorption contribution to the nonlinear optical response. Nonlinear scattering and nonlinear refraction effects, which can be present in particular at high fluences, were not recorded using this configuration.

As discussed earlier, the investigated [Py_8TPyzPzM] species can undergo aggregation in solution. The occurrence of aggregation can influence the dynamics of the excited states since different optical processes can be activated. Therefore, we recorded first the nonlinear transmittance of a 0.1 mM solution of the Mg^{II} complex, [Py_8TPyzPzMg-(H_2O)], in DMSO since in this solvent the complex shows an absence of aggregation; in addition, no changes are observed before and after the nonlinear optical experiment (figure not shown). Figure 10 reports the results which show that there is a decreasing transmittance for fluences higher than 100 mJ cm^{-2}, as expected for an RSA mechanism. The transmission data are reported using fluences (mJ cm^{-2}) and not intensities (mJ cm^{-2} s^{-1}) since the triplet states involved in the nonlinear process have lifetimes much longer than the 10 ns laser pulses used for the experiment.

The nonlinear transmittance of a 0.1 mM solution of the Zn^{II} complex in DMSO was also recorded. It is noteworthy

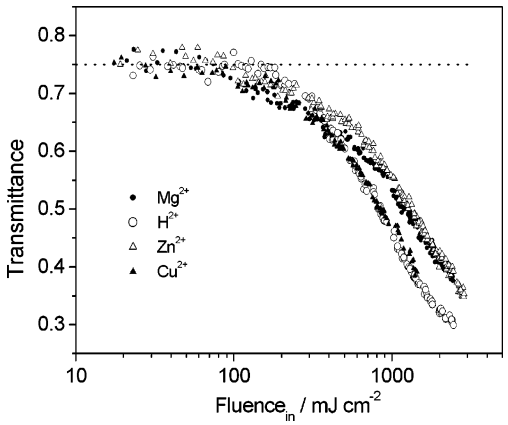

Figure 10. Nonlinear transmission measurements in open aperture configuration of 0.1 mM solutions of [Py_8TPyzPzM] (M = $2H^I$, $Mg^{II}(H_2O)$, Cu^{II}, Zn^{II}) in DMSO at 532 nm.

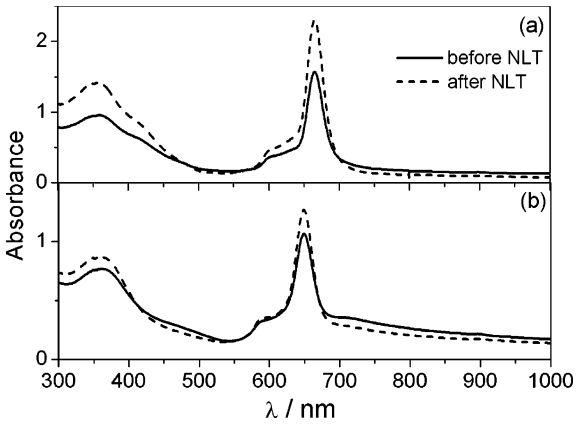

Figure 11. Absorbance of 0.1 mM solution of [Py_8TPyzPzM] (M = $2H^I$ (a), Cu^{II} (b)) in DMSO before and after nonlinear transmission measurements.

that, as for the Mg^{II} complex, the linear absorption spectrum indicates the presence of a monomeric Zn^{II} species and was found to be unchanged after the nonlinear optical experiment (spectrum not shown). From the plots of Figure 10, it can be seen that the nonlinear transmittance data for the Zn^{II} complex is very similar to that of the Mg^{II} complex. This indicates that the presence of a heavier metal center (Zn^{II}) which would favor intersystem crossing and a higher triplet population does not significantly influence the results.

The nonlinear transmittance of the unmetalated macrocycle present in DMSO in its deprotonated form, and of the Cu^{II} complex, which exhibit slower disaggregation kinetics, was also examined. Figure 11 shows that the linear absorption spectra of 0.1 mM solutions (initially not clear) of both species in DMSO undergo significant changes during the nonlinear optical experiment, indicating that disaggregation is taking place. The nonlinear transmittance data are compared in Figure 10 with those of the already mentioned Mg^{II} and Zn^{II} complexes. Clearly, for the free-base and Cu^{II} systems a larger nonlinear effect is observed, whereas, again, the latter two systems show a very similar behavior indicating that a variation of the intersystem crossing related to the central ion does not seem to be relevant. The nonlinear transmission of a more clear solution of the unmetalated macrocycle was also recorded (not shown in the figure), and

(22) (a) Perry, J. W. In *Nonlinear Optics of Organic Molecules and Polymers*; Nalwa, H. S., Miyata, S., Eds.; CRC: Boca Raton, FL, 1997; pp 813−840. (b) Hanack, M.; Schneider, T.; Barthel, M.; Shirk, J. S.; Flom, S. R.; Pong, R. G. S. *Coord. Chem. Rev.* **2001**, *219*−*221*, 235. (c) Nalwa, H. S.; Shirk, J. S. In *Phthalocyanines: Properties and Applications*; Leznoff, C. C., Lever, A. B. P., Eds.; VCH: Cambridge, U.K., 1996; Vol. 4, p 89. (d) Dini, D.; Barthel, M.; Hanack, M. *Eur. J. Org. Chem.* **2001**, 3759. Vagin, S.; Yang, G. Y.; Lee, M. K. Y.; Hanack, M. *Opt. Commun.* **2003**, *228*, 119.

its behavior was more similar to that of the nonaggregated Mg^{II} and Zn^{II} species. These results indicate that aggregation gives an important contribution to the multiphoton absorption mechanism.

On the basis of the nonlinear mechanism active for the present systems, namely the RSA involving excited triplet states, one can suggest that aggregation affects both the triplet state absorption cross section and the dynamics of excited state formation. This can induce different intersystem crossing efficiencies and, consequently, the overall efficiency of the multiphoton absorption process. Strong intermolecular interactions, like those present in the aggregated units, would give rise to more deactivation channels and therefore lead to a less efficient intersystem crossing. On the other hand, the interactions determine the cooperative effects which can be observed in the broadening of the transitions and also by some variation of the transition energies, as can be seen in the linear spectra. It can be suggested that the same effect is also present for the triplet to triplet transition and therefore that a variation of the absorption cross section at the frequency at which the nonlinear transmittance is measured can be expected. However, a lower intersystem crossing efficiency would determine a smaller nonlinear absorption. This is opposite to what is observed, since the aggregated species show a larger nonlinear transmittance. It is believed, therefore, that the most important effect would be a variation of the excited state properties which determines a larger excited state cross section of the triplet to triplet transition of the aggregate at 532 nm.

Although many factors can influence the multiphoton absorption,[21,22] it appears from the above results that aggregation plays a relevant role for the nonlinear optical behavior of the present macrocycles and a systematic study will be needed for understanding how the parameters, which are important for the multiphoton absorption process, are dependent on the intermolecular contacts in the aggregated species.

Conclusions

It was shown that a number of metal derivatives of general formula $[Py_8TPyzPzM]\cdot xH_2O$ ($M = Mg^{II}(H_2O)$, Mn^{II}, Co^{II}, Cu^{II}, Zn^{II}; $x = 3-8$) can be prepared under mild conditions and with good yields from the new "pyrazinoporphyrazine" macrocycle [$Py_8TPyzPzH_2$], described in part 1 of this series.[1] Different levels of electron withdrawing effects are expected to be present in this novel class of porphyrazine systems owing to the presence of the *meso* and the pyrazine N atoms and the N atoms present on the appended pyridine rings. The cumulative effect is such that the macrocycles can be more easily reduced than the related class of diazepinoporphyrazines or the phthalocyanine analogues and delocalization and redistribution of the excess of negative charge in the negatively charged systems $[Py_8TPyzPzM]^{n-}$ where $n = 1-4$ is strongly facilitated in the current investigated compounds. Moreover, the electrochemical measurements have also shown that the four reversible one-electron reductions are sensitive to the nature of the central metal ion and are favored in the sequence $Mg^{II}(H_2O) < Zn^{II} < Cu^{II} < Co^{II} < Mn^{II}$.

It appears plausible that the nonlinear optical data obtained for the [$Py_8TPyzPzM$] species ($M = Mg^{II}(H_2O)$, Zn^{II}, $2H^{I}$, Cu^{II}) can be interpreted in terms of a sequential two photon absorption mechanism. Nonlinear transmission measurements reveal that aggregation of the molecules can induce a variation of their nonlinear optical response. It is proposed that a cooperation mechanism is active for the aggregates since an increase of the excited state absorption cross section is found.

Acknowledgment. Financial support by the University of Rome La Sapienza, MIUR (Cofin 2003038084) and the Robert A. Welch Foundation (K.M.K, Grant E-680) is gratefully acknowledged. M.P.D. is indebted to the Department of Chemistry, The University of Houston, for generous help and kind hospitality. Thanks are expressed to Dr. P. A. Stuzhin (Ivanovo State University of Chemical Technology, Ivanovo, Russia) for critical comments and helpful suggestions and to Dr. Paola Galli and Dr. Jianming Lu for great experimental support.

Supporting Information Available: Figure S1, showing the spectral changes as a function of time for the Cu^{II} complex in different solvents. Table S1, reporting qualitative spectra in different solvents. This material is available free of charge via the Internet at http://pubs.acs.org.

IC0489084